Acta Geotechnica (2021) 16:1417–1427
https://doi.org/10.1007/s11440-020-01122-4

RESEARCH PAPER

Homogeneity and mechanical behaviors of sands improved by a temperature-controlled one-phase MICP method

Yang Xiao[1,2] · Yang Wang[2] · Shun Wang[3] · T. Matthew Evans[4] · Armin W. Stuedlein[4] · Jian Chu[5] · Chang Zhao[2] · Huanran Wu[1,2] · Hanlong Liu[1,2]

Received: 24 July 2020 / Accepted: 24 November 2020 / Published online: 2 January 2021

Abstract
Microbially induced carbonate precipitation (MICP) has been actively investigated as a promising method to improve soil properties. A burning issue impeding its wide application is the severe spatial inhomogeneity of the $CaCO_3$ distribution. Inspiring by the temperature sensitivity of the bacteria activity, a temperature-controlled one-phase MICP method is proposed consisting of two major steps: (1) grouting the specimen with the mixture of cementation and bacteria solutions in a low temperature; (2) inducing $CaCO_3$ precipitation by exposing the specimen to room temperature. A series of experiments are conducted to demonstrate the advantages of the proposed method over the normal two-phase MICP method. Specimens treated with the proposed temperature-controlled method present higher $CaCO_3$ contents with a roughly uniform distribution along the height of the specimen; the strength of those specimens are substantially improved with apparent dilatancy due to the effective bond network formed by the homogeneously distributed $CaCO_3$ precipitation. SEM images indicate that the temperature-controlled method tends to form small crystals distributing uniformly on the grain surface, which may increase the roughness of the grain and the residual stress more effectively.

Keywords Homogeneity · MICP · Quartz sand · Strength · Temperature

1 Introduction

Microbially induced carbonate precipitation (MICP) [21, 40, 55, 59, 90, 91] is a promising technique to improve soils with carbonate precipitation induced by environment-friendly ureolytic bacteria, filling the void space among soil grains, increasing roughness of the grain surfaces and forming effective bonds at interparticle contacts [3, 17, 22, 30, 32, 33, 47, 48, 50, 57, 59, 89]. The carbonate ions are induced from urea by the bacteria and the carbonate precipitation can form if calcium ions are supplied [21, 40, 66, 97]:

$$CO(NH_2)_2 + H_2O \xrightarrow{\text{ureolytic bacteria}} 2NH_4^+ + CO_3^{2-} \quad (1)$$

$$CO_3^{2-} + Ca^{2+} \rightarrow CaCO_3 \downarrow \quad (2)$$

Many experimental investigations have been conducted on MICP-treated soil specimens, demonstrating an improvement in strength, stiffness, dilatancy and liquefaction resistance [8, 15, 18, 20, 21, 25, 26, 34, 36, 46, 49, 51, 57, 63, 67–69, 77, 78, 81, 82, 87, 88, 94, 95, 100, 101, 104, 106, 108, 111, 112], a decrease in hydraulic conductivity [3, 5, 7, 9, 15, 16, 19, 24, 36, 37, 39, 42, 43, 53, 58, 73, 76, 83, 84, 98, 99], and restraint of particle breakage [107]. The effect of MICP treatment might be influenced by base material factors (e.g., mineralogy, grain shape, grain roughness, gradation, fines content, relative density of the sand specimen, etc.)

✉ Huanran Wu
hwucqu@163.com

[1] Key Laboratory of New Technology for Construction of Cities in Mountain Area, Chongqing University, Chongqing 400045, China

[2] School of Civil Engineering, Chongqing University, Chongqing 400045, China

[3] Institute of Geotechnical Engineering, University of Natural Resources and Life Sciences, Vienna, Austria

[4] School of Civil and Construction Engineering, Oregon State University, Corvallis, OR, USA

[5] School of Civil and Environmental Engineering, Nanyang Technological University, Singapore 639798, Singapore

[9, 29, 31, 37, 52, 58, 60, 63, 70–72, 79–81, 92, 106, 113], bacterial, chemical and technical factors (e.g., bacterial concentration, bacterial type, composition and concentration of the cementation solution, clay nucleation, flow rate, injection times and intervals, one-phase or multiple-phase method, pH, temperature, etc.) [1, 2, 10, 13, 14, 17, 27, 53, 54, 56, 61, 62, 64, 73, 76, 86, 96, 105, 113]. A critical issue encountered in these experiments is the inhomogeneity of the MICP-treated specimen. It is often reported that a majority of carbonate precipitates close to the inlet area of the chemical reaction solution [8, 10, 25, 48], and the spatial inhomogeneity increases substantially with increasing concentration of reaction solutions [8, 41]. The potential reason might be the inhomogeneous convection and diffusion of the bacteria and reaction solutions in the grouting stage [64, 85, 90, 97].

It is reported that the activity of the bacteria might be influenced by ambient conditions including temperature and pH of the bio-mixture solution [11, 105]. Biochemistry experiments showed that the optimum temperature of urease activity was about 30 °C [65, 66]. Production rate of $CaCO_3$ increased from 20 to 30 °C for bacteria and from 10 to 60 °C for urease enzyme. Further experiments [10] reported that larger clusters consisting of calcium carbonate crystals could be formed at lower temperature and better improve the strength of the specimens. Given the temperature-sensitivity of the activity of the bacteria, a novel and effective approach is proposed to improve the homogeneity of the MICP-treated specimen, i.e., dispersing the mixture of bacteria and reaction solutions in low temperatures to achieve a relatively uniform condition for the MICP process. A series of experiments are conducted, to evaluate the homogeneity and mechanical responses of the specimens, and to demonstrate the advantages of the proposed temperature-controlled method over the normal two-phase method (i.e., staged injection method [12]).

2 Methodology

2.1 Test materials

Fujian quartz sands with the grain size distribution as shown in Fig. 1a, b were adopted in the current study as the tested material, whose maximum and minimum void ratios were 0.978 and 0.523, respectively. The sands were packed into a plastic tube to form a cylindrical specimen, whose diameter was 39.1 mm and height was 80 mm. An undercompaction method proposed by Ladd [45] was adopted to obtain consistent and uniform sand specimens [6, 35, 38, 74, 75, 102, 103, 109, 110]. The oven-dried sands mixed with 5% de-aired water were divided into six equal parts. Every part was placed into the mold in sequence and compacted slightly more in density (about 1%) than its substratum. The prepared specimen had a relative density of 40–45%.

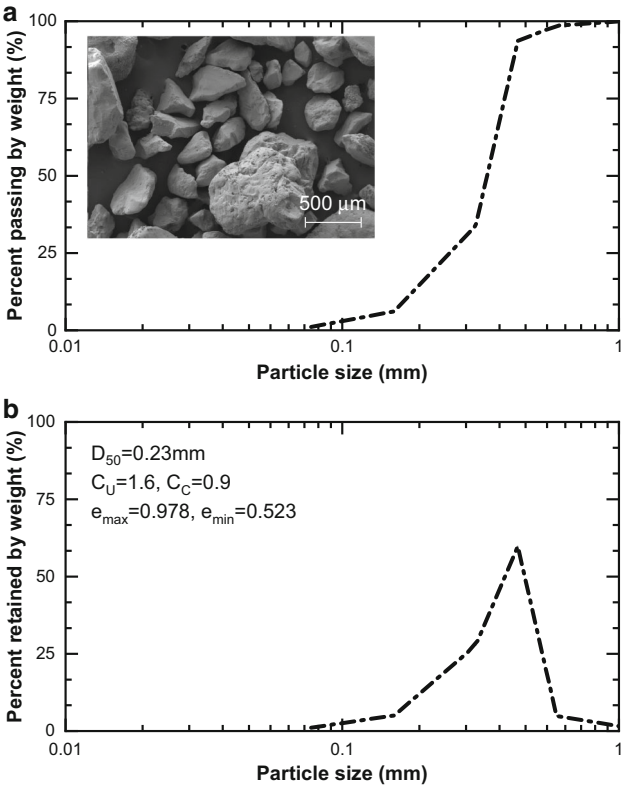

Fig. 1 Particle size distribution of the silica sands prior to loading in terms of **a** percent passing by weight (data from [93]), **b** percent retained by weight

2.2 Temperature-controlled MICP method

Sporosarcina pasteurii (DSM 33; ATCC 11859), a widely adopted ureolytic bacterium [3, 16], was employed in the current study. In the typical two-phase MICP method [14, 44], the bacteria and reaction solutions are usually grouted into the specimen from top to bottom under gravity [23, 36]. $CaCO_3$ precipitation would be first induced at the top of the specimen, leading to a decrease in hydraulic conductivity and preventing the subsequent solutions from transporting downwards. An inhomogeneous MICP-treated specimen would be formed as a consequence, with a majority of $CaCO_3$ precipitation close to the grouting inlet. It has been reported that the distribution of $CaCO_3$ depends on particle size distribution, relative density of the sand specimen, concentrations of the solutions and flow rate [3, 10].

A possible way to improve the homogeneity of $CaCO_3$ precipitation in MICP-treated specimen is to inhibit the activity of the bacteria and distribute the mixture of bacteria and cementation solutions uniformly prior to MICP reaction. The urease activities of the bacteria solution at various

temperatures are measured with a conductivity method [97] to investigate its temperature-sensitivity. Interested readers please refer to [93] for more details about the measurement. Figure 2a shows clearly an almost constant activity at temperatures of 17–22 °C and a peak urease activity at a temperature around 33 °C. It is interesting to note that the urease activity decreases with decreasing temperature for temperatures below 16 °C; the urease activity decreases to around zero at temperatures around 10 °C, i.e., $CaCO_3$ precipitation is inhibited in that temperature, which could be chosen as the controlling state.

In view of the low activity of urea-hydrolytic bacteria in low temperatures, a temperature-controlled one-phase MICP method (TCOP) is proposed to achieve a homogenous MICP-treated specimen, which consists of: (1) grouting with the mixture of bacteria and cementation solutions in low temperatures; (2) inducing $CaCO_3$ precipitation in relatively high temperatures. Specifically, in the current study, the bacteria solution (20 mL, optical density OD_{600} = 1.628 ~ 1.753) and cementation solutions (250 mL, consisting of equimolar $CaCl_2$ and urea) were first mixed and kept in 10 °C with a temperature controller. Then, the mixture was grouted into the sand specimen, placed horizontally, by a pump at a steady velocity (5.0 mL/min) to achieve a relatively uniform distribution. Specimens with different MICP-treatment levels were obtained by varying the concentration of the cementation solution (0.5, 1.0, 2.0 M). A typical room-temperature two-phase MICP method (RTTP) is adopted as well for comparison. In this scheme, 20 mL bacteria solution was grouted into the specimen first at a steady velocity (5.0 mL/min), followed by 250 mL cementation solution at the same velocity at room temperature (26 °C). After the grouting steps, the cementation liquid was retained in the specimen for 10 h in both TCOP and RTTP treatment procedures.

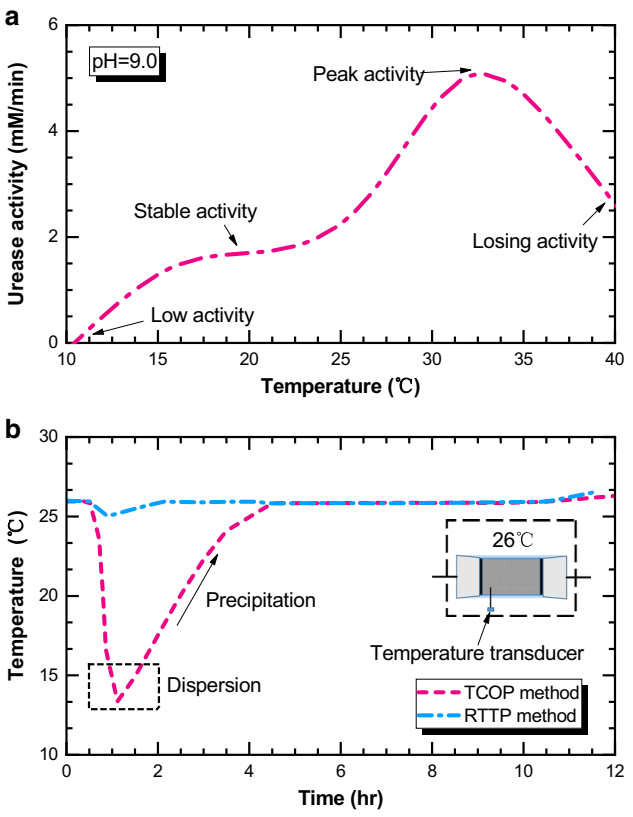

Fig. 2 **a** Evolution of urease activity for *Sporosarcina pasteurii* (DSM 33; ATCC 11859) with varied temperature (adapted from [93]), **b** temperature histories for specimens treated with TCOP and RTTP methods

Temperature evolutions were recorded, with a transducer embedded into the specimen (see the inset in Fig. 2b), for the proposed TCOP method and typical RTTP method, respectively. As shown in Fig. 2b, the temperature in the specimen treated with the TCOP method drops remarkably to around 13 °C during the grouting stage, as compared to the almost constant temperature around 26 °C in the one treated with the RTTP method. The temperature could be maintained below 15 °C for around 1.0 h in the TCOP method, suggesting the inhibited activity of the bacteria during the grouting stage. The sand specimen, exposed to a room temperature of 26 °C, is heated thereafter through the thermal transmission. The ureolytic bacteria are activated at the same time, hydrolyzing urea and inducing $CaCO_3$ precipitation.

2.3 *Evaluation of strength and $CaCO_3$ distribution*

Triaxial compression tests were conducted to examine the mechanical properties of the MICP-treated specimens. When moved into the triaxial apparatus, the specimens were placed in a way that the part close to the solution inlet is on the top. The specimens were saturated under an effective confining pressure of 10 kPa, with an increasing back pressure until the pore pressure coefficient reached 0.96. Then, the specimens were isotropically consolidated under an effective confining pressure of 20 kPa and subjected to axial load with a constant vertical displacement rate of 0.1 mm/min under drained condition afterward.

After the triaxial compression tests, the distribution of $CaCO_3$ was evaluated to estimate the homogeneity of MICP-treated specimens. Samples were obtained from different positions (top: close to the solution inlet, middle, bottom: close to the outlet) of the specimens and $CaCO_3$ contents were evaluated with the typical acid-washing method [41, 48, 97]. The $CaCO_3$ contents could be calculated as follows:

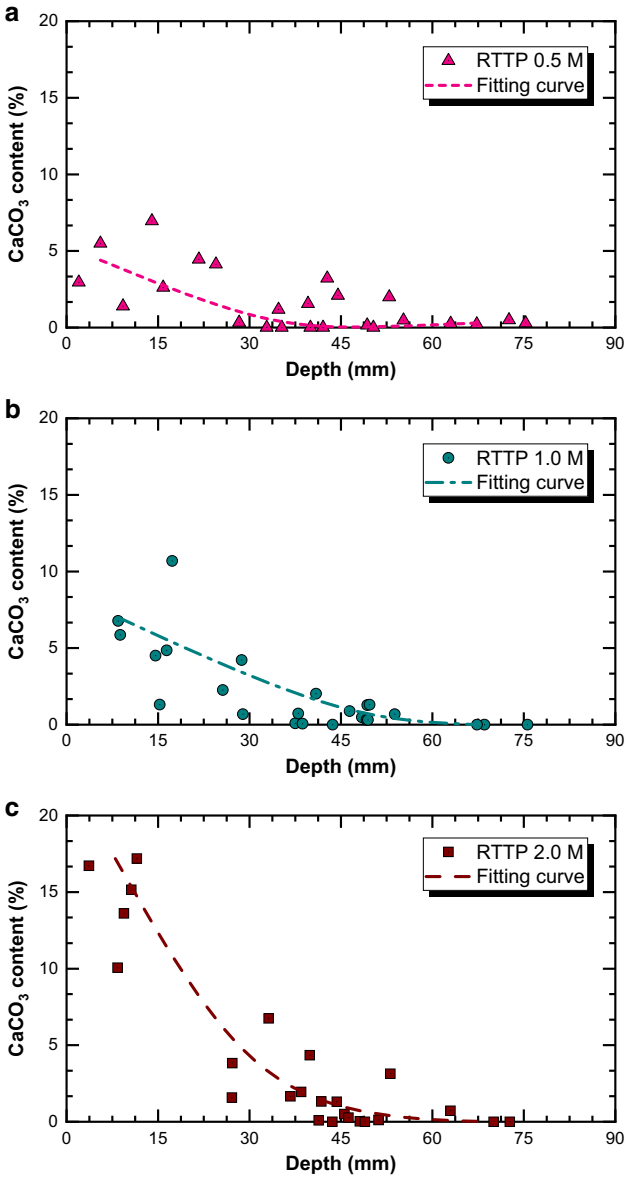

Fig. 3 $CaCO_3$ distribution along the height of the specimen for RTTP-treated specimens with **a** 0.5 M, **b** 1.0 M and **c** 2.0 M cementation solutions

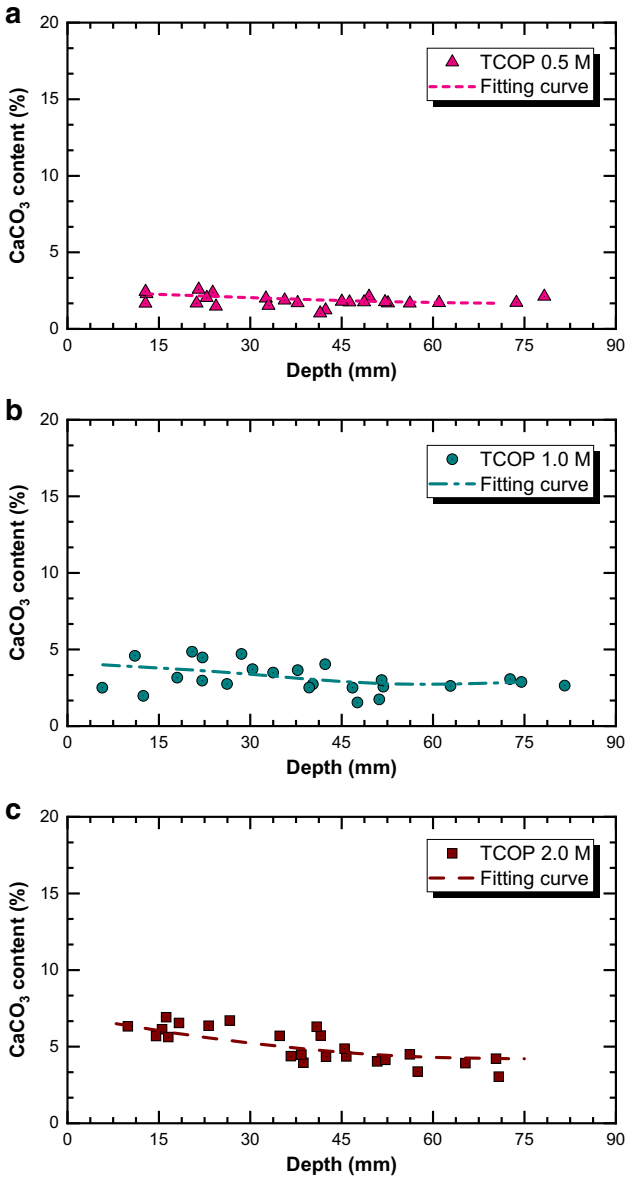

Fig. 4 $CaCO_3$ distribution along the height of the specimen for TCOP-treated specimens with **a** 0.5 M, **b** 1.0 M and **c** 2.0 M cementation solutions

$$C_{ca} = \frac{m_0 - m_1}{m_0} \times 100\% \quad (3)$$

where m_0 is the dry weight of the sample before acid-washing; m_1 is the dry weight of the sample after acid-washing. SEM images were captured to observe the microscale distribution of $CaCO_3$ precipitation.

3 Results and discussions

3.1 *Distribution of $CaCO_3$ precipitation*

Figures 3 and 4 show $CaCO_3$ content distributions for RTTP-treated and TCOP-treated specimens treated with cementation solutions of different concentrations (0.5, 1.0, 2.0 M), respectively. Note that repetitive tests have been conducted for every concentration condition to increase the reliability of the data. The $CaCO_3$ content decreases from top to bottom in RTTP-treated specimens. $CaCO_3$ could be rarely found at the bottom for all cases treated with 0.5 M

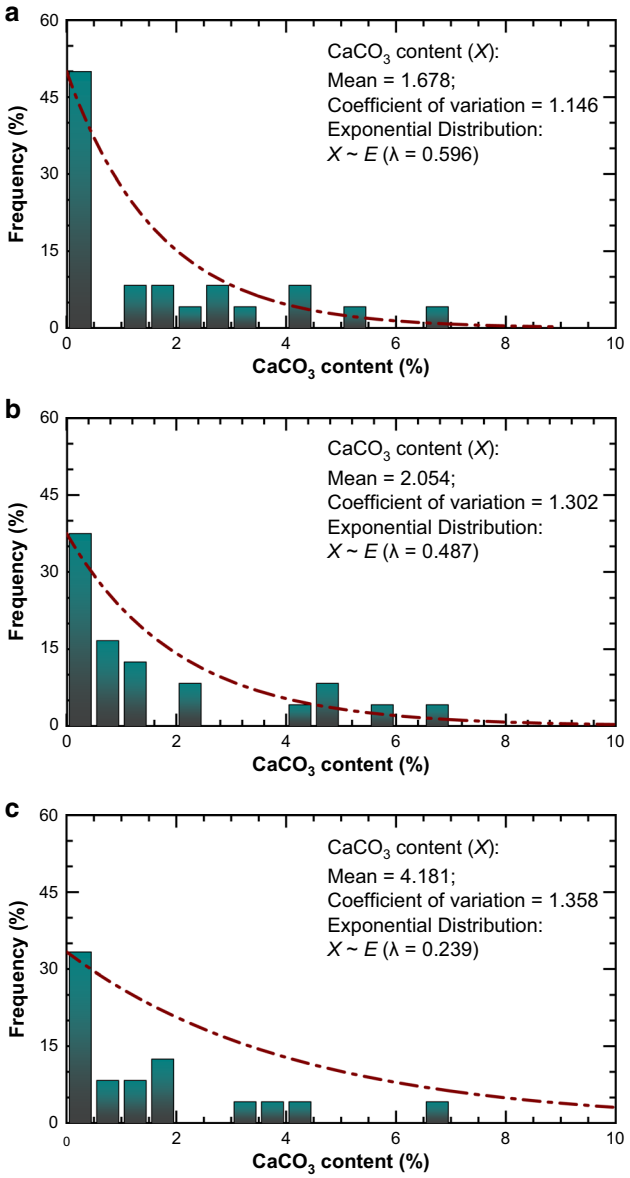

Fig. 5 Probability distribution of $CaCO_3$ content and curve fitting with exponential distribution for RTTP-treated specimens with **a** 0.5 M, **b** 1.0 M and **c** 2.0 M cementation solutions

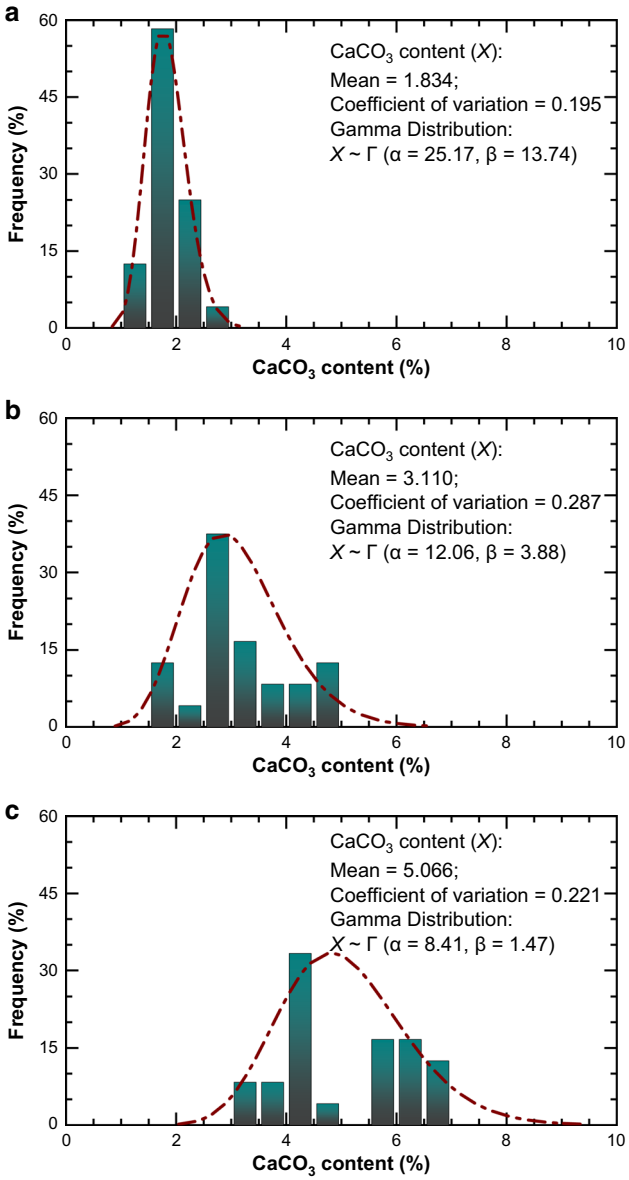

Fig. 6 Probability distribution of $CaCO_3$ content and curve fitting with Gamma distribution for TCOP-treated specimens with **a** 0.5 M, **b** 1.0 M and **c** 2.0 M cementation solutions

reaction solutions as shown in Fig. 3a. Even if treated with cementation solutions of a higher concentration, the $CaCO_3$ contents at the bottom can barely increase as shown in Fig. 3b, c. On the contrary, $CaCO_3$ contents for the TCOP-treated specimens present largely uniform distributions; the $CaCO_3$ contents, at both the top and the bottom of the specimens, increase effectively with increasing concentration of the reaction solution as shown in Fig. 4a–c.

To better interpret the spatial distribution of $CaCO_3$, the probability distributions of $CaCO_3$ content for RTTP-treated and TCOP-treated specimens have been presented in Figs. 5 and 6, respectively. It is noted that the $CaCO_3$ content (X) of RTTP-treated specimens roughly obeys an exponential distribution function:

$$f(x;\lambda) = \lambda e^{-\lambda x} \quad \text{for } x \geq 0 \text{ and } \lambda > 0 \tag{4}$$

where $\lambda > 0$ is the rate parameter. In contrast, the $CaCO_3$ content of TCOP-treated specimens roughly follows a Gamma distribution:

$$f(x;\alpha,\beta) = \frac{\beta^{\alpha} x^{\alpha-1} e^{-\beta x}}{\Gamma(\alpha)} \quad \text{for } x > 0 \text{ and } \alpha,\ \beta > 0 \tag{5}$$

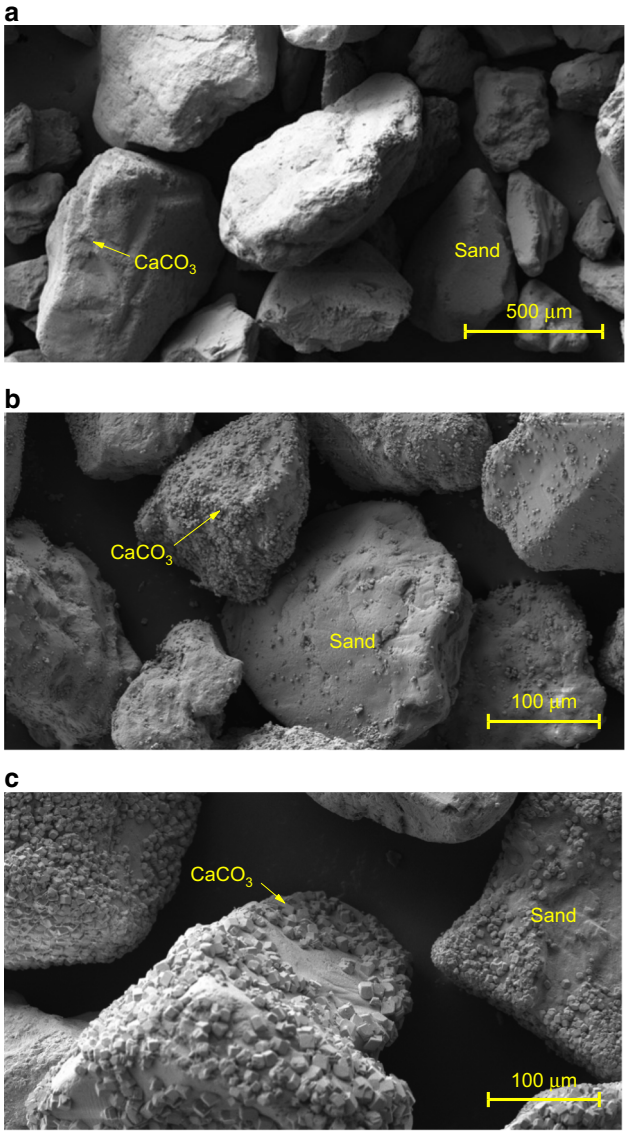

Fig. 7 SEM images for RTTP-treated specimens with **a** 0.5 M, **b** 1.0 M and **c** 2.0 M cementation solutions

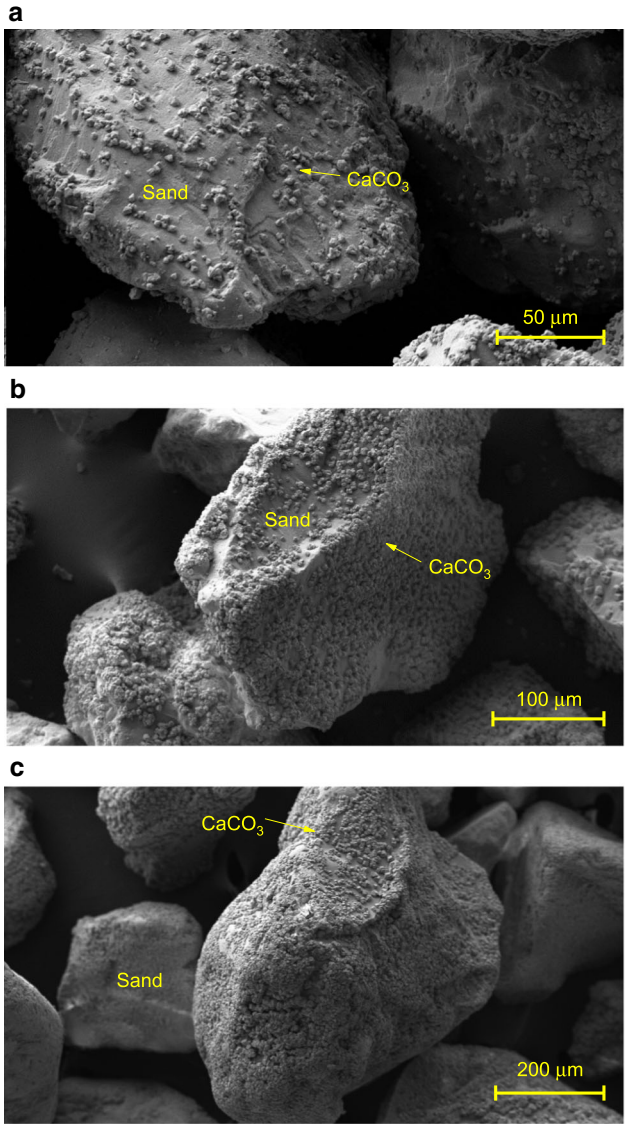

Fig. 8 SEM images for TCOP-treated specimens with **a** 0.5 M, **b** 1.0 M and **c** 2.0 M cementation solutions

where $\Gamma(\alpha)$ is the complete gamma function, α is the shape parameter, and β is the rate parameter. The corresponding fitting curves with key parameters are presented in Figs. 5 and 6.

The mean and the coefficients of variation (the standard deviation divided by the mean) calculated based on the raw data are presented in every subplot as well. An increase in mean content with increasing chemical concentration is observed for RTTP-treated (from 1.678 to 4.181 as in Fig. 5) and TCOP-treated (from 1.834 to 5.066 as in Fig. 6) specimens, respectively. Moreover, for specimens treated with cementation solutions of the same concentration, the TCOP method could yield a higher mean content as compared with the RTTP method, e.g., $CaCO_3$ content of 4.181 for RTTP-treated specimens (see Fig. 5c) versus 5.066 for TCOP-treated specimens (see Fig. 6c), both treated with 2.0 M reaction solutions. More importantly, the coefficients of variation for TCOP-treated specimens (0.195 to 0.287 in Fig. 6) are substantially lower than those for RTTP-treated ones (1.146 to 1.358 Fig. 5), indicating a considerable improvement in homogeneity of the MICP-treated specimens by adopting the TCOP method. In brief, the TCOP method enables both a more efficient $CaCO_3$ precipitation and an improved homogeneity of the specimen, suggesting the potential to provide a more effective and controllable MICP technique for relevant engineering applications.

Figures 7 and 8 show the SEM images of samples from the center of the RTTP-treated and TCOP-treated

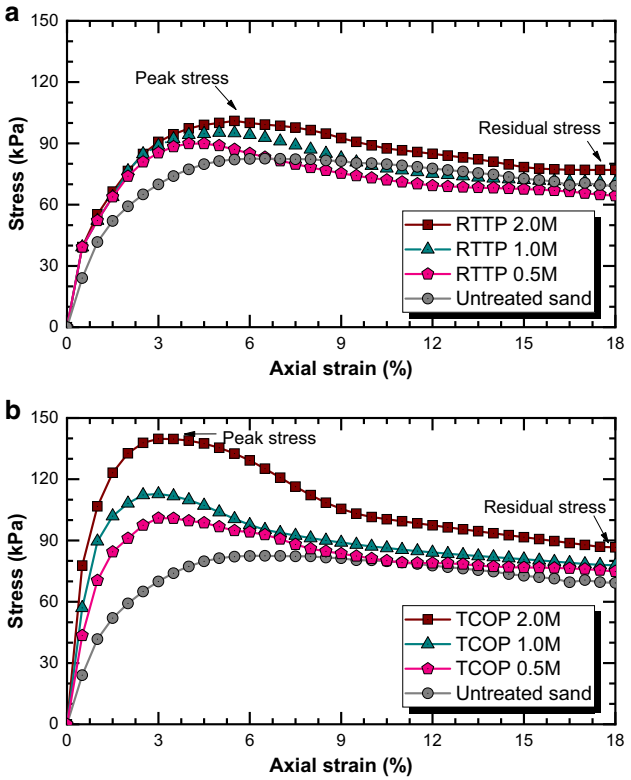

Fig. 9 Stress–strain relations in drained triaxial compression tests for **a** RTTP-treated specimens and **b** TCOP-treated specimens (data for untreated sand from [93])

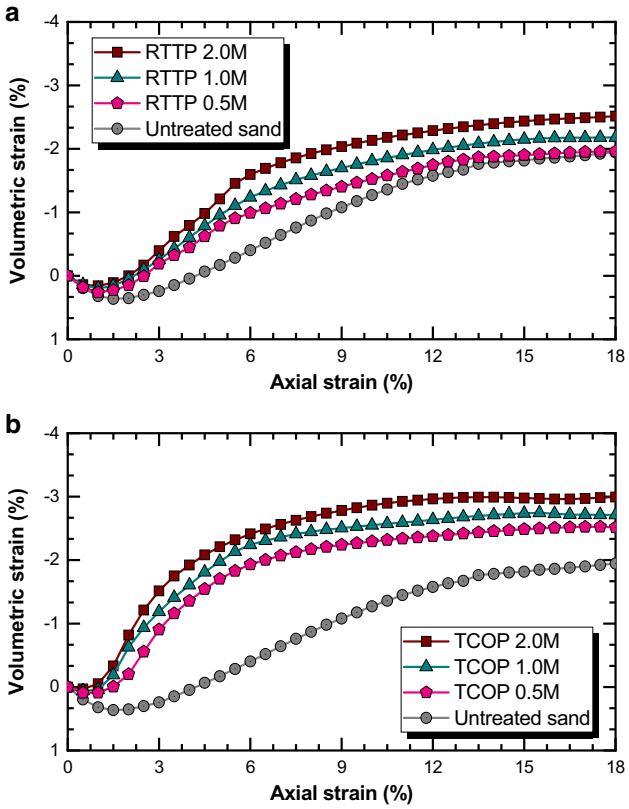

Fig. 10 Evolutions of volumetric strain in drained triaxial compression tests for **a** RTTP-treated specimens and **b** TCOP-treated specimens (data for untreated sand from [93])

specimens, respectively. It is observed that the crystal morphology is indeed affected by the temperature history of the MICP process. In the RTTP-treated samples, $CaCO_3$ tends to form larger $CaCO_3$ crystals with increasing chemical concentration (see Fig. 7a–c). Specifically, it is noted that $CaCO_3$ prefers to precipitate on particles with an irregular surface comparing with those smooth ones, as shown in Fig. 7b. On the contrary, small $CaCO_3$ crystals distribute largely uniformly among various particles under TCOP conditions; more crystals of similar size are formed with increasing chemical concentrations, covering the surfaces of grains (see Fig. 8a–c). This interesting phenomenon can be attributed to the temperature-controlled history which helps avoid the spatial heterogeneity within the specimen and enables a favorable dynamic crystallization condition on the surfaces of sand particles [104].

3.2 Drained triaxial tests

The average stress–strain relations over the repetitive tests for specimens treated with RTTP method and TCOP method are presented in Fig. 9. Slight increases in initial stiffness and peak stress are observed in Fig. 9a for RTTP-treated specimens. By comparison, increases in initial stiffness and peak stress are substantial for TCOP-treated specimens as shown in Fig. 9b. The improvements in peak stress and initial stiffness become more significant with the increase in the concentration of the cementation solution for TCOP-treated specimens. Note the clear shear softening behaviors for the one treated with a 2.0 M reaction solution. The evolutions of volumetric strain with axial strain are displayed in Fig. 10. Notably, the TCOP method leads to a more significant increase in volume dilation than the RTTP method; the maximum dilation rates are larger and appear earlier in the TCOP-treated specimens than in the RTTP-treated ones.

The relationships between the peak stress and the average $CaCO_3$ content of the specimen are shown in Fig. 11a. The peak stress for untreated sand (85 kPa) is presented as the gray dashed line for reference. Repetitive tests have been conducted to verify our observations and every point on the figure represents an individual test. The peak stresses for RTTP-treated specimens are slightly larger than that for the untreated sand and a marginal increase is noted with the increase in $CaCO_3$ content. The maximum peak stress for RTTP-treated specimens (treated with 2.0 M reaction solution) is around 110 kPa. In contrast, the increases in peak stress for TCOP-treated specimens are

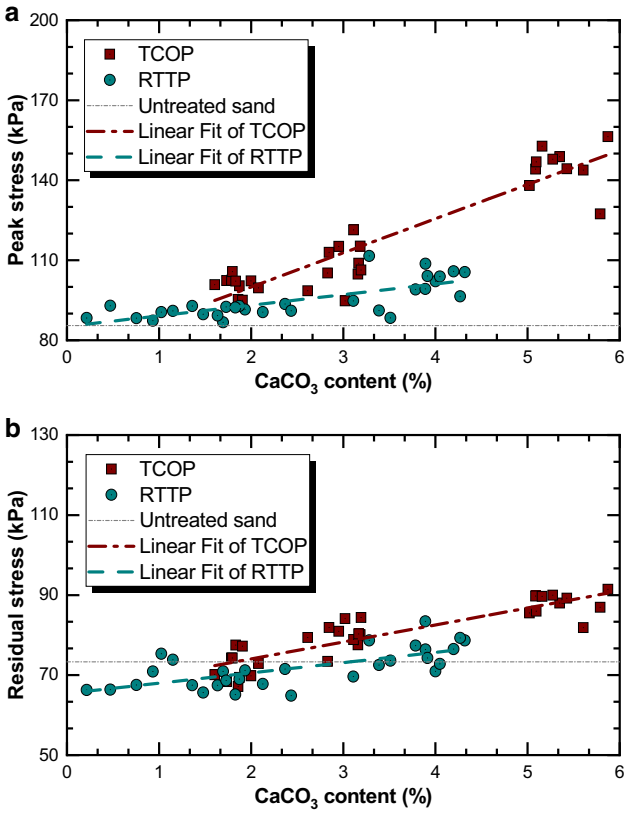

Fig. 11 Variations of **a** peak stress and **b** residual stress with $CaCO_3$ content for TCOP-treated and RTTP-treated specimens

substantially larger and the increase with increasing $CaCO_3$ content is more distinct. Notably, the maximum peak stress for TCOP-treated specimens (treated with 2.0 M reaction solution) is around 160 kPa (around twice as high as that for untreated sand). This is attributed to the homogenous distribution of $CaCO_3$ within the TCOP-treated specimens, which forms effective interparticle bond networks. By comparison, the larger crystals in RTTP-treated specimens (see Fig. 7c) does not lead to significantly more effective strength improvement. The dominating factor herein is the homogeneity of the $CaCO_3$ distribution. $CaCO_3$ distributes mainly on the top of the RTTP-treated specimens (see Fig. 3) and cannot reinforce the bottom section effectively. Therefore, the overall strength of the specimens, controlled by the weakest part, cannot be increased considerably.

The relationships between the residual stress and the average $CaCO_3$ content of the specimen are presented in Fig. 11b, with a grey dashed line indicating that for untreated sand (73 kPa). It is surprising to note the general decrease (with several increasing cases) in residual stress for specimens with low $CaCO_3$ contents ($< 2.5\%$), treated with both RTTP and TCOP methods. The residual stress could be reduced to as low as 65 kPa. This counterintuitive phenomenon, verified by repetitive tests, is attributable to the apparent shear bands (a strain-localized failure pattern during the triaxial shearing process [4, 28]), where the overall regularity of the grains increases due to a small amount of $CaCO_3$ precipitation filling the concave on the grain surface [105]. This speculation is supported by previous SEM images presenting a preference of $CaCO_3$ precipitating on the grains with relatively irregular surfaces. In comparison, the specimens with higher $CaCO_3$ contents ($> 2.5\%$) tend to present a higher residual stress; and the increase by the TCOP method is more effective (maximum around 90 kPa). As supported by the micro-scale observations from the SEM images, the overall roughness of the grain surfaces would increase due to the increase in amount/size of $CaCO_3$ crystals with increasing $CaCO_3$ content, leading to the higher residual stresses.

4 Conclusions

A temperature-controlled one-phase (TCOP) MICP method is proposed to improve the homogeneity of MICP-treated sands. The advantages of the proposed TCOP method are demonstrated with distributions of $CaCO_3$ and evolutions of strength and dilatancy, as compared with the normal room-temperature two-phase (RTTP) MICP method. Major findings are summarized below:

1. $CaCO_3$ tends to precipitate in the upper part of the RTTP-treated specimens, with almost no $CaCO_3$ in the bottom part. On the contrary, under conditions with the same bacteria and cementation solutions, the TCOP method generally produces more $CaCO_3$ precipitation with a much lower spatial variation, presenting a roughly uniform distribution of $CaCO_3$ along the height of the specimen.
2. Specimens treated with the TCOP method display apparent strain-softening behaviors with intense dilation responses. The peak stress increases substantially with $CaCO_3$ content for the TCOP-treated specimens (as high as 160 kPa) as compared with the marginal increase for the RTTP-treated ones (maximum around 110 kPa). This difference is attributed to the effective bond network formed by the homogenously distributed $CaCO_3$ precipitation within the TCOP-treated specimen, as compared with the inhomogeneous distribution of $CaCO_3$ within the RTTP-treated specimen, leaving a barely reinforced bottom section.
3. It is surprising that specimens with lower $CaCO_3$ content ($< 2.5\%$) present lower residual stresses as compared with the untreated sands. This phenomenon is attributable to the increase in overall regularity of the grains (in the apparent shear bands) due to a small amount of $CaCO_3$ precipitation. Higher $CaCO_3$ content

(> 2.5%) could still increase the residual stress due to the increase in roughness of the grain surfaces (in the apparent shear bands), and TCOP method is more effective thanks to the small crystals uniformly distributed among different grains.

Acknowledgments The authors would like to acknowledge the financial support from the National Natural Science Foundation of China (Grant Nos. 41831282, 51922024 and 52078085) and Natural Science Foundation of Chongqing, China (Grant No. cstc2019j-cyjjqX0014). T. Matthew Evans was supported by the National Science Foundation (NSF) (Grant No. CMMI-1933355) during this work.

References

1. Akiyama M, Kawasaki S (2019) Biogeochemical simulation of microbially induced calcite precipitation with *Pararhodobacter* sp. strain so1. Acta Geotech 14:685–696
2. Al QA et al (2012) Factors affecting efficiency of microbially induced calcite precipitation. J Geotech Geoenviron Eng 138:992–1001
3. Al QA, Soga K (2013) Effect of chemical treatment used in micp on engineering properties of cemented soils. Géotechnique 63:331–339
4. Alikarami R et al (2015) Strain localisation and grain breakage in sand under shearing at high mean stress: insights from in situ x-ray tomography. Acta Geotech 10:15–30
5. Amini KM et al (2019) Comparison of effects of different nutrients on stimulating indigenous soil bacteria for biocementation. J Mater Civil Eng 31:04019067
6. Amini F, Qi GZ (2000) Liquefaction testing of stratified silty sands. J Geotech Geoenviron Eng 126:208–217
7. Botusharova S et al (2020) Augmenting microbially induced carbonate precipitation of soil with the capability to self-heal. J Geotech Geoenviron Eng 146:04020010
8. Burbank M et al (2013) Geotechnical tests of sands following bioinduced calcite precipitation catalyzed by indigenous bacteria. J Geotech Geoenviron Eng 139:928–936
9. Cheng L et al (2013) Cementation of sand soil by microbially induced calcite precipitation at various degrees of saturation. Can Geotech J 50:81–90
10. Cheng L et al (2017) Influence of key environmental conditions on microbially induced cementation for soil stabilization. J Geotech Geoenviron Eng 143:04016083
11. Cheng L et al (2019) Soil bio-cementation using a new one-phase low-ph injection method. Acta Geotech 14:615–626
12. Cheng L, Cord-Ruwisch R (2012) In situ soil cementation with ureolytic bacteria by surface percolation. Ecol Eng 42:64–72
13. Cheng L, Shahin MA (2016) Urease active bioslurry: a novel soil improvement approach based on microbially induced carbonate precipitation. Can Geotech J 53:1376–1385
14. Choi S-G et al (2016) Biocementation for sand using an eggshell as calcium source. J Geotech Geoenviron Eng 142:06016010
15. Chou C-W et al (2011) Biocalcification of sand through ureolysis. J Geotech Geoenviron Eng 137:1179–1189
16. Chu J et al (2013) Microbial method for construction of an aquaculture pond in sand. Géotechnique 63:871–875
17. Chu J et al (2014) Optimization of calcium-based bioclogging and biocementation of sand. Acta Geotech 9:277–285
18. Cui M et al (2017) Influence of cementation level on the strength behaviour of bio-cemented sand. Acta Geotech 12:971–986
19. Dadda A et al (2017) Characterization of microstructural and physical properties changes in biocemented sand using 3d x-ray microtomography. Acta Geotech 12:955–970
20. Darby KM et al (2019) Centrifuge model testing of liquefaction mitigation via microbially induced calcite precipitation. J Geotech Geoenviron Eng 145:04019084
21. DeJong JT et al (2006) Microbially induced cementation to control sand response to undrained shear. J Geotech Geoenviron Eng 132:1381–1392
22. DeJong JT et al (2010) Bio-mediated soil improvement. Ecol Eng 36:197–210
23. Du Y-J et al (2013) Stress–strain relation and strength characteristics of cement treated zinc-contaminated clay. Eng Geol 167:20–26
24. Farah T et al (2016) Durability of bioclogging treatment of soils. J Geotech Geoenviron Eng 142:04016040
25. Feng K, Montoya BM (2016) Influence of confinement and cementation level on the behavior of microbial-induced calcite precipitated sands under monotonic drained loading. J Geotech Geoenviron Eng 142:04015057
26. Feng K, Montoya BM (2017) Quantifying level of microbial-induced cementation for cyclically loaded sand. J Geotech Geoenviron Eng 143:06017005
27. Ferris FG et al (2004) Kinetics of calcite precipitation induced by ureolytic bacteria at 10 to 20 degrees c in artificial groundwater. Geochim Cosmochim Acta 68:1701–1710
28. Finno RJ, Rechenmacher AL (2003) Effects of consolidation history on critical state of sand. J Geotech Geoenviron Eng 129:350–360
29. Gao Y et al (2019) Mechanical behaviour of biocemented sands at various treatment levels and relative densities. Acta Geotech 14:697–707
30. Gomez MG et al (2015) Field-scale bio-cementation tests to improve sands. Proc Inst Civ Eng Ground Improv 168:206–216
31. Gomez MG et al (2017) Large-scale comparison of bioaugmentation and biostimulation approaches for biocementation of sands. J Geotech Geoenviron Eng 143:04016124
32. Gomez MG et al (2018) Stimulation of native microorganisms for biocementation in samples recovered from field-scale treatment depths. J Geotech Geoenviron Eng 144:04017098
33. Gomez MG et al (2019) Biogeochemical changes during biocementation mediated by stimulated and augmented ureolytic microorganisms. Sci Rep 9:11517
34. Haryati Y et al (2018) Review on biological process of soil improvement in the mitigation of liquefaction in sandy soil. MATEC Web Conf 250:01017
35. Hazirbaba K, Rathje EM (2009) Pore pressure generation of silty sands due to induced cyclic shear strains. J Geotechn Geoenviron Eng 135:1892–1905
36. He J, Chu J (2014) Undrained responses of microbially desaturated sand under monotonic loading. J Geotech Geoenviron Eng 140:04014003
37. Hoang T et al (2019) Sand and silty-sand soil stabilization using bacterial enzyme–induced calcite precipitation (beicp). Can Geotech J 56:808–822
38. Høeg K et al (2000) Strength of undisturbed versus reconstituted silt and silty sand specimens. J Geotech Geoenviron Eng 126:606–617
39. Ivanov V et al (2019) Biocementation technology for construction of artificial oasis in sandy desert. J King Saud Univ Eng Sci 3463298. https://doi.org/10.1016/j.jksues.2019.07.003
40. Ivanov V, Chu J (2008) Applications of microorganisms to geotechnical engineering for bioclogging and biocementation of soil in situ. Rev Environ Sci Biotechnol 7:139–153
41. Jiang NJ et al (2016) Multi-scale laboratory evaluation of the physical, mechanical, and microstructural properties of soft

highway subgrade soil stabilized with calcium carbide residue. Can Geotech J 53:373–383
42. Jiang N-J et al (2017) Microbially induced carbonate precipitation for seepage-induced internal erosion control in sand–clay mixtures. J Geotech Geoenviron Eng 143:04016100
43. Jiang N-J, Soga K (2017) The applicability of microbially induced calcite precipitation (micp) for internal erosion control in gravel–sand mixtures. Géotechnique 67:42–55
44. Kang X et al (2016) Cement hydration-based micromechanics modeling of the time-dependent small-strain stiffness of fly ash-stabilized soils. Int J Geomech 16:10
45. Ladd RS (1978) Preparing test specimens using undercompaction. Geotech Test J 1:16–23
46. Li M et al (2016) Influence of fiber addition on mechanical properties of micp-treated sand. J Mater Civil Eng 28:04015166
47. Li C et al (2019) Sulfate acid corrosion mechanism of biogeomaterial based on micp technology. J Mater Civil Eng 31:04019097
48. Lin H et al (2016) Mechanical behavior of sands treated by microbially induced carbonate precipitation. J Geotech Geoenviron Eng 142:04015066
49. Liu L et al (2019) Strength, stiffness, and microstructure characteristics of biocemented calcareous sand. Can Geotech J 56:1502–1513
50. Liu S et al (2020) Effectiveness of the anti-erosion of an micp coating on the surfaces of ancient clay roof tiles. Constr Build Mater 243:118202
51. Ma G et al (2020) Strength and permeability of bentonite-assisted biocemented coarse sand. Can Geotech J. https://doi.org/10.1139/cgj-2020-0045
52. Mahawish A et al (2018) Effect of particle size distribution on the bio-cementation of coarse aggregates. Acta Geotech 13:1019–1025
53. Martinez BC et al (2013) Experimental optimization of microbial-induced carbonate precipitation for soil improvement. J Geotech Geoenviron Eng 139:587–598
54. Minto JM et al (2019) Development of a reactive transport model for field-scale simulation of microbially induced carbonate precipitation. Water Resour Res 55:7229–7245
55. Mitchell AC, Ferris FG (2006) The influence of bacillus pasteuriion the nucleation and growth of calcium carbonate. Geomicrobiol J 23:213–226
56. Mitchell JK, Santamarina JC (2005) Biological considerations in geotechnical engineering. J Geotech Geoenviron Eng 131:1222–1233
57. Montoya BM et al (2013) Dynamic response of liquefiable sand improved by microbial-induced calcite precipitation. Géotechnique 63:302–312
58. Montoya BM et al (2019) Enhancement of coal ash compressibility parameters using microbial-induced carbonate precipitation. J Geotech Geoenviron Eng 145:04019018
59. Montoya BM, DeJong JT (2015) Stress–strain behavior of sands cemented by microbially induced calcite precipitation. J Geotech Geoenviron Eng 141:04015019
60. Morales L et al (2015) Feasibility of a soft biological improvement of natural soils used in compacted linear earth construction. Acta Geotech 10:157–171
61. Mortensen BM et al (2011) Effects of environmental factors on microbial induced calcium carbonate precipitation. J Appl Microbiol 111:338–349
62. Mujah D et al (2019) Microstructural and geomechanical study on biocemented sand for optimization of micp process. J Mater Civil Eng 31:04019025
63. Nafisi A et al (2020) Shear strength envelopes of biocemented sands with varying particle size and cementation level. J Geotech Geoenviron Eng 146:04020002
64. Nassar MK et al (2018) Large-scale experiments in microbially induced calcite precipitation (micp): Reactive transport model development and prediction. Water Resour Res 54:480–500
65. Nemati M et al (2005) Permeability profile modification using bacterially formed calcium carbonate: comparison with enzymic option. Process Biochem 40:925–933
66. Nemati M, Voordouw G (2003) Modification of porous media permeability, using calcium carbonate produced enzymatically in situ. Enzyme Microb Technol 33:635–642
67. O'Donnell TS et al (2017) Midp: liquefaction mitigation via microbial denitrification as a two-stage process. Ii: Micp. J Geotech Geoenviron Eng 143:04017095
68. O'Donnell TS et al (2017) Midp: liquefaction mitigation via microbial denitrification as a two-stage process. I: desaturation. J Geotech Geoenviron Eng 143:04017094
69. O'Donnell TS, Kavazanjian E (2015) Stiffness and dilatancy improvements in uncemented sands treated through micp. J Geotech Geoenviron Eng 141:02815004
70. Oliveira PJV et al (2017) Effect of soil type on the enzymatic calcium carbonate precipitation process used for soil improvement. J Mater Civil Eng 29:04016263
71. Pan X et al (2020) A new biogrouting method for fine to coarse sand. Acta Geotech 15:1–16
72. Park S-S et al (2014) Effect of plant-induced calcite precipitation on the strength of sand. J Mater Civil Eng 26:06014017
73. Pham VP et al (2018) Evaluating strategies to improve process efficiency of denitrification-based micp. J Geotech Geoenviron Eng 144:04018049
74. Polito CP et al (2008) Pore pressure generation models for sands and silty soils subjected to cyclic loading. J Geotech Geoenviron Eng 134:1490–1500
75. Polito CP, Martin JR II (2001) Effects of nonplastic fines on the liquefaction resistance of sands. J Geotech Geoenviron Eng 127:408–415
76. Proto CJ et al (2016) Biomediated permeability reduction of saturated sands. J Geotech Geoenviron Eng 142:04016073
77. Riveros GA, Sadrekarimi A (2020) Liquefaction resistance of fraser river sand improved by a microbially-induced cementation. Soil Dyn Earthq Eng 131:106034
78. Riveros GA, Sadrekarimi A (2020) Effect of microbially-induced cementation on the instability and critical state behaviors of fraser river sand. Can Geotech J. https://doi.org/10.1139/cgj-2019-0514
79. Rowshanbakht K et al (2016) Effect of injected bacterial suspension volume and relative density on carbonate precipitation resulting from microbial treatment. Ecol Eng 89:49–55
80. Safavizadeh S et al (2018) Microbial induced calcium carbonate precipitation in coal ash. Géotechnique 69:727–740
81. Sasaki T, Kuwano R (2016) Undrained cyclic triaxial testing on sand with non-plastic fines content cemented with microbially induced $caco_3$. Soils Found 56:485–495
82. Simatupang M et al (2018) Small-strain shear modulus and liquefaction resistance of sand with carbonate precipitation. Soil Dyn Earthq Eng 115:710–718
83. Song CP et al (2019) The influence of particle morphology on microbially induced $caco_3$ clogging in granular media. Mar Georesour Geotechnol. https://doi.org/10.1080/1064119X.1062019.1677828
84. Soon NW et al (2014) Factors affecting improvement in engineering properties of residual soil through microbial-induced calcite precipitation. J Geotech Geoenviron Eng 140:04014006
85. Stocks-Fischer S et al (1999) Microbiological precipitation of $caco_3$. Soil Biol Biochem 31:1563–1571
86. Sun X et al (2019) Study of the effect of temperature on microbially induced carbonate precipitation. Acta Geotech 14:627–638

87. Tagliaferri F et al (2011) Observing strain localisation processes in bio-cemented sand using x-ray imaging. Granul Matter 13:247–250
88. Terzis D, Laloui L (2019) Cell-free soil bio-cementation with strength, dilatancy and fabric characterization. Acta Geotech 14:639–656
89. van Paassen LA et al (2010) Potential soil reinforcement by biological denitrification. Ecol Eng 36:168–175
90. van Paassen LA et al (2010) Quantifying biomediated ground improvement by ureolysis: large-scale biogrout experiment. J Geotech Geoenviron Eng 136:1721–1728
91. van Paassen LA et al (2010) Biogrout, ground improvement by microbial induced carbonate precipitation. Ph.d., thesis, Delft University of Technology, Delft
92. Venda OP, Neves JPG (2019) Effect of organic matter content on enzymatic biocementation process applied to coarse-grained soils. J Mater Civil Eng 31:04019121
93. Wang Y et al (2018) Study on low-strength biocemented sands using a temperature-controlled micp (microbially induced calcite precipitation) method. In: Proceedings of the 5th GeoChina international conference, pp 15–26
94. Wang K et al (2020) Stress-strain behaviour of bio-desaturated sand under undrained monotonic and cyclic loading. Géotechnique. https://doi.org/10.1680/jgeot.1619.P.1080
95. Wang X, Tao J (2018) Polymer-modified microbially induced carbonate precipitation for one-shot targeted and localized soil improvement. Acta Geotech 14:657–671
96. Wen K et al (2019) Development of an improved immersing method to enhance microbial induced calcite precipitation treated sandy soil through multiple treatments in low cementation media concentration. Geotech Geol Eng 37:1015–1027
97. Whiffin VS et al (2007) Microbial carbonate precipitation as a soil improvement technique. Geomicrobiol J 24:417–423
98. Wu C et al (2019) 3d characterization of microbially induced carbonate precipitation in rock fracture and the resulted permeability reduction. Eng Geol 249:23–30
99. Wu C et al (2019) Microbially induced calcite precipitation along a circular flow channel under a constant flow condition. Acta Geotech 14:673–683
100. Xiao P et al (2018) Liquefaction resistance of bio-cemented calcareous sand. Soil Dyn Earthq Eng 107:9–19
101. Xiao Y et al (2019) Unconfined compressive and splitting tensile strength of basalt fiber-reinforced biocemented sand. J Geotech Geoenviron Eng 145:04019048
102. Xiao Y et al (2019) Effect of particle shape on stress-dilatancy responses of medium-dense sands. J Geotech Geoenviron Eng 145:04018105
103. Xiao Y et al (2019) Thermal conductivity of sand-tire shred mixtures. J Geotech Geoenviron Eng 145:06019012
104. Xiao P et al (2019) Effect of relative density and bio-cementation on the cyclic response of calcareous sand. Can Geotech J 56:1849–1862
105. Xiao Y et al (2019) Strength and deformation responses of biocemented sands using a temperature-controlled method. Int J Geomech 19:04019120
106. Xiao Y et al (2019) Effect of particle shape on strength and stiffness of biocemented glass beads. J Geotech Geoenviron Eng 145:06019016
107. Xiao Y et al (2020) Restraint of particle breakage by biotreatment method. J Geotech Geoenviron Eng 146:04020123
108. Xiao Y et al (2020) Toe bearing capacity of precast concrete piles through biogrouting improvement. J Geotech Geoenviron Eng 146:06020026
109. Yamamuro JA, Covert KM (2001) Monotonic and cyclic liquefaction of very loose sands with high silt content. J Geotech Geoenviron Eng 127:314–324
110. Yang SL et al (2006) Instability of sand-silt mixtures. Soil Dyn Earthq Eng 26:183–190
111. Zamani A, Montoya BM (2018) Undrained monotonic shear response of micp-treated silty sands. J Geotech Geoenviron Eng 144:04018029
112. Zamani A, Montoya BM (2019) Undrained cyclic response of silty sands improved by microbial induced calcium carbonate precipitation. Soil Dyn Earthq Eng 120:436–448
113. Zhao Q et al (2014) Factors affecting improvement of engineering properties of micp-treated soil catalyzed by bacteria and urease. J Mater Civil Eng 26:04014094